HSPI The Open Access Publisher

ICCI INSIGHTS IN CLINICAL AND CELLULAR IMMUNOLOGY
ISSN 2640-2793

Research Article

Modulation of atrial natriuretic peptide receptors in ovarian folliculogenesis

Sung Zoo Kim*

Department of Physiology, Jeonbuk National University Medical School, Gungiro 20, Jeonju-54907, Republic of Korea

Abstract

Specific receptors for atrial natriuretic peptide (ANP) located in intra-ovarian tissues are suggested to be involved in ovarian functions such as oocyte maturation and follicle development. However, the characteristics and modulation of its receptor in relation to ovarian folliculogenesis are not well defined. This study examined the properties of ANP receptors in the ovary using quantitative receptor autoradiography. In the pig ovary, the highest binding sites for ^{125}I-ANP$_{(1-28)}$ were localized in the granulosa cell layer of the follicles as well as cumulus oophorous. The binding sites for ^{125}I-ANP$_{(1-28)}$ on theca layer of the ovarian follicles were mainly localized in the external layer, but none was observed in the internal layer. Specific binding of ^{125}I-ANP$_{(1-28)}$ was not found clearly in atretic follicles. In the corpus luteum, the binding site was not observed. Analysis of the competitive inhibition of the binding of ^{125}I-ANP$_{(1-28)}$ to the granulosa and theca externa layers in various preovulatory follicles by increasing concentrations of unlabeled ANP$_{(1-28)}$ was consistent with a single high affinity for ^{125}I-ANP$_{(1-28)}$. The maximal binding capacities of ^{125}I-ANP$_{(1-28)}$ in granulosa layer were significantly increased in proportion to the development of ovarian follicles. However, no significant difference of binding capacities of ^{125}I-ANP$_{(1-28)}$ was observed in theca externa layer. The binding affinities of ^{125}I-ANP$_{(1-28)}$ in granulosa and theca externa layers were not different from each other. Especially, the correlation between specific binding of ^{125}I-ANP$_{(1-28)}$ and follicle diameter. A significant correlation was revealed between specific binding of ^{125}I-ANP$_{(1-28)}$ and follicle diameter ($R = 0.88$, $p < 0.0001$) in granulosa layer, however, less relationship was detected in theca externa layer ($R = 0.50$, $p < 0.0001$). Therefore, these results indicate that the biological ANP receptors exist in granulosa and the theca externa layers of the pig ovary, and suggest that the ANP receptors in granulosa layer may be related to the regulatory function of the ovarian follicullogenesis including oocyte maturation.

More Information

***Address for Correspondence:** Sung Zoo Kim, Ph.D., Department of Physiology, JeonBuk National University, Medical School, Gungiro 20, Jeonju 54907, Republic of Korea, Email: szkim@jbnu.ac.kr

Submitted: January 02, 2022
Approved: January 21, 2022
Published: January 24, 2022

How to cite this article: Kim SZ. Modulation of atrial natriuretic peptide receptors in ovarian folliculogenesis. Insights Clin Cell Immunol. 2022; 6: 001-007.

DOI: 10.29328/journal.icci.1001019

Copyright License: © 2022 Kim SZ. This is an open access article distributed under the Creative Commons Attribution License, which permits unrestricted use, distribution, and reproduction in any medium, provided the original work is properly cited.

Keywords: Natriuretic peptide receptor; Autoradiography; Granulosa layer; Pig ovary

Check for updates

OPEN ACCESS

Introduction

In mammals, it is well demonstrated that ovaries are composed of various follicles, which are basic functional units. Also, ovary is an extremely dynamic organ in which a large majority of follicles are effectively eliminated throughout their reproductive life. The total number of follicles in the ovary is determined early in life, and the depletion of this pool leads to reproductive senescence [1]. The mechanisms regulating follicular growth and atresia in mammalian ovaries have been clarified, not only their systemic regulation by gonadotropins but also their intra-ovarian regulation by gonadal steroids, growth factors, cytokines and intracellular proteins [2]. Most of the studies on ovarian folliculogenesis are focused on the development of early antral follicles to the preovulatory stage, leading to the successful use of exogenous follicle stimulating hormone (FSH) for infertility treatment. Accumulating data indicate that preantral follicles are under stringent regulation by FSH and local intra-ovarian factors, thus providing the possibility to develop new therapeutic approaches [3].

The natriuretic peptide family consists of three biologically active peptides: atrial natriuretic peptide (ANP), brain natriuretic peptide (BNP), and C-type natriuretic peptide (CNP). Among these, ANP and BNP are secreted by the heart and act as cardiac hormones. Both ANP and BNP preferentially bind to natriuretic peptide receptor-A (NPR-A) and exert similar effects through increases in intracellular cyclic guanosine monophosphate (cGMP) within target tissues [4,5]. Although it was originally isolated from rat atria, ANP is not confined to cardiac tissue but is also found in a number of extra-atrial tissues and organs. Earlier studies have demonstrated the presence of immunoreactive ANP in the intra-ovarian tissues found in the bovine [6] and rat [7]. The

identification of mRNA encoding ANP in the granulosa cells of the pig ovary suggested that the ovarian granulosa cells could be the site for the synthesis and secretion of ANP [8,9]. It is therefore suggested that the intra-ovarian ANP system may be closely related with the ovarian functions including follicular development and oocyte maturation.

In previous studies, the presence of specific binding sites for ANP has been found in several ovarian tissues of mammals; in the preovulatory follicles of human [10], the cultured human granulosa luteal cells [11], the bovine corpus luteum [6] and the pig granulosa cells [12]. And mRNA encoding NPR is located in all regions of the granulosa compartment, but not in the oocyte [13,14]. NPR mRNA is more concentrated in the cumulus cell region and in the region of the mural granulosa closest to the antral space. Liu, et al. [15] reported the regulatory functions of natriuretic peptide precursor C (NPPC) and NPR2 in maintaining oocyte meiotic arrest and discuss the possibility that LH could stimulate meiotic resumption by decreasing NPPC content and NPR2 activity. Taken together, these findings appear to demonstrate that NPR serves as a key control system during folliculogenesis and oocyte maturation. However, the cellular distribution of the receptors for ANP in the ovarian tissues have not yet been clarified. The purpose of the present study was to define the morphological and quantitative characteristics of NPRs on intra-ovarian structures using *in vitro* receptor autoradiography, and to examine the relation to follicular development in porcine ovary.

Materials and methods

Collection of ovaries and preparation of cryostat sections

For *in vitro* receptor autoradiography, ovaries from healthy young pigs were collected at a slaughterhouse within 10 min of slaughter, and were immediately snap-frozen in isopentane cooled by dry ice, and stored in sealed boxes at -70 °C prior to frozen sectioning. Serial 20-µm sections were cut on a cryostat at -20 °C, thaw-mounted onto gelatin–chrom–alum coated slides, and dried in a desiccator at 4° overnight before immediate incubation [16].

Preparation of radioligands

The iodinated ^{125}I-ANP$_{(1-28)}$ was prepared as described previously [17]. In brief, 5 µg of synthetic ANP$_{(1-28)}$ (Peninsula, Belmont, CA) were introduced into a vial containing 25 µl of 0.5 M phosphate-buffered saline (pH 7.4) followed by the addition of 1 mCi of Na^{125}I (Amersham, Little Chalfont, UK). Chloramine-T (10 µg per 10 µl) was added to the reaction vial and mixed gently, and 30 seconds later, the reaction was terminated by bovine serum albumin (BSA) solution (60 mg/200 ml).

The reaction mixture was immediately applied to an elution column (Sephadex G-25; Sigma, Poole, UK) and eluted with 0.1 M acetic acid containing 0.3% BSA, 0.3% lysozyme, 0.1% glycine, and 200 Kallikrein inhibiting units per milliliter aprotinin. The iodinated ANP$_{(1-28)}$ was repurified by reversed-phase HPLC on an elution (µBondapak) column with a linear gradient of 20% to 60% acetonitrile in 0.1% TFA. The specific activity (approximately 1,750 Ci/mmol) of ^{125}I-ANP$_{(1-28)}$ was determined by radioimmunoassay technique [18].

In vitro autoradiographic binding of ^{125}I-ANP$_{(1-28)}$

Incubation with ^{125}I-ANP$_{(1-28)}$ was performed as previously reported [19, 20]. Briefly, the sections were washed with 150 mM NaCl-0.5% acetic acid (pH 5.0) at room temperature for 10 min in order to remove endogenous ANP, and then preincubated with 30 mM phosphate buffer (pH 7.2) containing 120 mM NaCl and 1 mM phenanthroline at room temperature for 10 min. The sections were incubated with ^{125}I-ANP$_{(1-28)}$ in fresh preincubation buffer containing 40 µg/ml bacitracin, 100 µg/ml phenylmethylsulfonyl fluoride, 10 µg/ml leupeptin, and 0.5% BSA at room temperature. After incubation, the sections were rinsed and washed with fresh preincubation buffer for 5 min at 4 °C. Subsequently, they were rinsed three times in cold distilled water at 4 °C and quickly dried under a stream of cold air. In preliminary experiments, the time course of the specific binding of the radioligand was established in the presence or absence of excess unlabeled ANP$_{(1-28)}$. The saturable specific binding of ^{125}I-ANP$_{(1-28)}$ was assessed in serial sections which were incubated with increasing concentrations (0 - 750 pM) of the radioligand in the presence or absence of 1 µM ANP$_{(1-28)}$. Competitive inhibition of the binding of ^{125}I-ANP$_{(1-28)}$ was examined in consecutive sections by coincubating with various concentrations of unlabeled ANP$_{(1-28)}$. To test the specificity of ^{125}I-ANP$_{(1-28)}$ binding, adjacent sections were incubated in the presence of the unrelated peptides, angiotensin II or arginine vasopressin (all 10 µM).

Microdensitometry of autoradiograms

Autoradiographic images were generated by exposing sections to Hyperfilm-^{3}H (Amersham International plc, Buckinghamshire, U.K.) in X-ray cassettes together with 20 µm-thick ^{125}I-labeled polymer standard strips (Amersham International plc) at room temperature for 7 days. Autoradiograms were developed in Kodak D-19 developer (Eastman Kodak Co., Rochester, NY) for 3 min and fixed in Kodak rapid fixer for 5 min at room temperature. Sections were then fixed in formaldehyde and stained with hematoxylin and eosin [19,20].

Autoradiographic images were viewed with a Leica Wild M420 Macroscope, and captured using a Sony video camera with CCD iris and a Hamamatsu AC adaptor connected to a Power Macintosh 8100/80AV computer. Regional binding of ^{125}I-ANP$_{(1-28)}$ in the ovary was analyzed using the PRISM image program (Version 3.6-1, Improve Vision, Coventry, UK). Optical densities were measured as disintegrations per minute (dpm) per square millimeter, based on the comparison with the calibration curve derived from the autoradiograms of

the ^{125}I standard microscales included in each X-ray cassette. These data were converted into femtomoles ^{125}I-ANP$_{(1-28)}$ bound per square millimeter, as described elsewhere [21].

The number of ligand binding sites of different affinities, their apparent dissociation constants (K_d) and their maximal binding capacities (B_{max}) on particular structures were derived separately in each individual using the LIGAND iterative model-fitting computer program [22].

Statistical analysis

Data show the results (means ± SE values) of individual experiments. Comparisons of results were performed by paired Student's t - test and ANOVA with Duncan multiple range tests, accepting $p < 0.05$ as the criterion of significance. Statistical analysis was performed using Graph Pad Prism software 7 (GraphPad Software, La Jolla, CA, USA).

Results

Specific ^{125}I-ANP$_{(1-28)}$ binding sites were demonstrated in the pig ovarian tissues using quantitative *in vitro* autoradiographic technique.

As shown in Figure 1A, the comparison of autoradiograms with their corresponding hematoxylin-eosin stained sections revealed typically specific reversible bindings of ^{125}I-ANP$_{(1-28)}$ with high densities to the granulosa cell layer of preovulatory follicles in the pig ovary. A low density of binding sites was revealed in the theca externa layer of the antral follicles, while the binding was not observed in the theca interna layer and the interstitial region of the ovary. In the presence of 1 μM unlabeled ANP$_{(1-28)}$ the bindings to the granulosa and theca externa layers of follicles were completely displaced, but the diffuse background bindings were not affected (Figure 1B). Ten micromolar unrelated peptides including angiotensin II and arginine vasopressin did not displace the binding of ^{125}I-ANP$_{(1-28)}$ at either granulosa or theca externa layers of follicles (data not shown). These binding properties of ^{125}I-ANP$_{(1-28)}$ on granulosa and theca externa layer were confirmed by autoradiograms combined with histological staining using emulsion-coated slides (Figure 2).

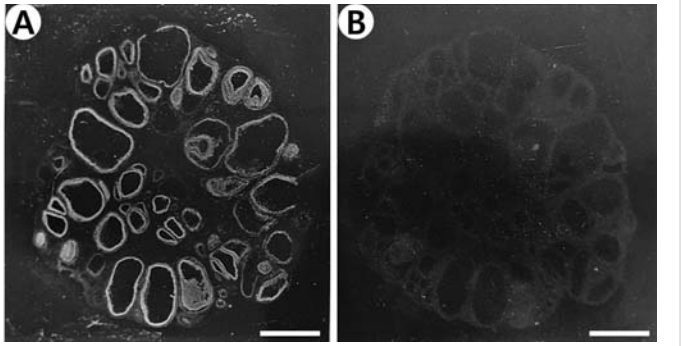

Figure 1: Dark-field photomicrograph of autoradiograms of the pig ovarian sections incubated in the presence of 250 pM ^{125}I-ANP$_{(1-28)}$ (A) and its adjacent section incubated in 250 pM ^{125}I-ANP$_{(1-28)}$ plus 1 μM unlabeled ANP$_{(1-28)}$ (B). ^{125}I-ANP$_{(1-28)}$ binding sites appear as white silver grains. Bars = 3 mm.

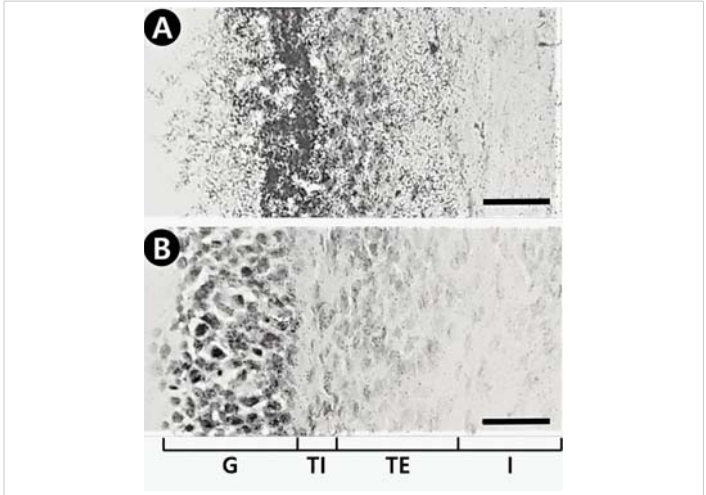

Figure 2: Autoradiographs combined with histological staining showing that specific grains of ^{125}I-ANP$_{(1-28)}$ are localized on the granulosa (G) and the theca externa (TE) layers of the follicles, but none in the theca interna (TI) layer and the interstitial tissues (I). Pig ovarian tissue sections were labeled and exposed to emulsion-coated slides. A, total binding; B, nonspecific binding. Bars = 40 μm.

There are various localization of specific ^{125}I-ANP$_{(1-28)}$ binding sites in several developmental stages of follicles. Firstly specific ^{125}I-ANP$_{(1-28)}$ binding site in the primary follicles was only noticed in granulosa layer (Figure 1A). Following the follicles were surrounded by the theca folliculi, specific ^{125}I-ANP$_{(1-28)}$ binding sites were founded in the theca externa layer as well as in the granulosa layer (Figures 3,4). In the large antral follicles, specific ^{125}I-ANP$_{(1-28)}$ binding was also found in the cumulus oophorous, a hillock of granulosa cells. But ^{125}I-ANP$_{(1-28)}$ binding sites were absent in the ovum (Figures 3,4). As shown in Figure 4B, specific binding of ^{125}I-ANP$_{(1-28)}$ was not found clearly in atretic follicles. Total bindings of ^{125}I-ANP$_{(1-28)}$ were shown in the corpus luteum (Figure 5A), but these bindings did not displaced by excess concentrations (1 μM) of unlabeled ANP$_{(1-28)}$, pBNP$_{(1-26)}$ or C-ANP (Figure 5).

In the pig ovary, different binding densities of ^{125}I-ANP$_{(1-28)}$ between granulosa and theca externa layers were found. As shown in Figure 6, specific binding to ovarian follicles was much higher in granulosa than in theca externa layer. Analysis of the competitive inhibition by unlabeled ANP$_{(1-28)}$ of the binding of ^{125}I-ANP$_{(1-28)}$ on granulosa and theca externa layers was consistent with reversible binding sites for ANP$_{(1-28)}$ of uniform affinity on each structure. As shown in Table 1, maximal binding capacities of ^{125}I-ANP$_{(1-28)}$ in granulosa layer were significantly increased in proportion to follicle diameter, the development of ovarian follicles. However, no significant difference of binding capacities of ^{125}I-ANP$_{(1-28)}$ was observed in theca externa layer. The binding affinities of ^{125}I-ANP$_{(1-28)}$ in granulosa and theca externa layers were approximately 2-3 nM, and these values were not different from each other. Figure 7 shows the correlation between specific binding of ^{125}I-ANP$_{(1-28)}$ and follicle diameter. A significant correlation was revealed between specific binding of ^{125}I-ANP$_{(1-28)}$ and follicle diameter ($R = 0.88$, $p < 0.0001$) in granulosa layer, however, less relationship was detected in theca externa layer ($R = 0.50$, $p < 0.0001$).

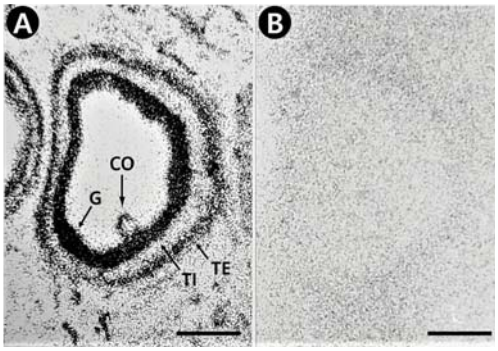

Figure 3: Light-field photomicrograph of autoradiograms showing that specific grains are localized on the granulosa (G), cumulus oophorous (CO) and the theca externa (TE) layers in the large antral follicles of the pig ovarian sections, but none in the theca interna (TI) layer. ^{125}I-ANP$_{(1-28)}$ binding sites appear as black silver grains. A, total binding; B, nonspecific binding. Bars = 500 μm.

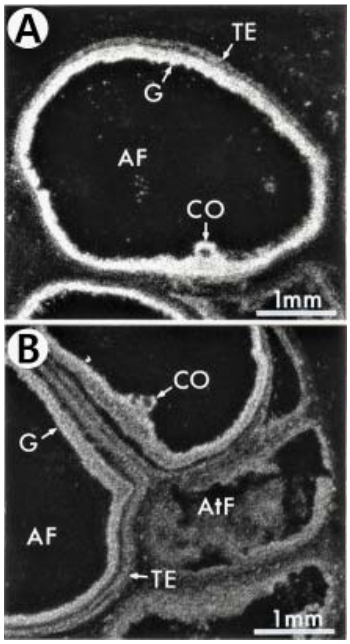

Figure 4: Dark-field photomicrograph of autoradiograms showing that specific grains are localized on the granulosa (G), cumulus oophorous (CO) and the theca externa (TE) layers in the large antral follicles (AF) of the pig ovarian sections (A and B), but not clear on the atretic follicle (AtF) (B). ^{125}I-ANP$_{(1-28)}$ binding sites appear as white silver grains.

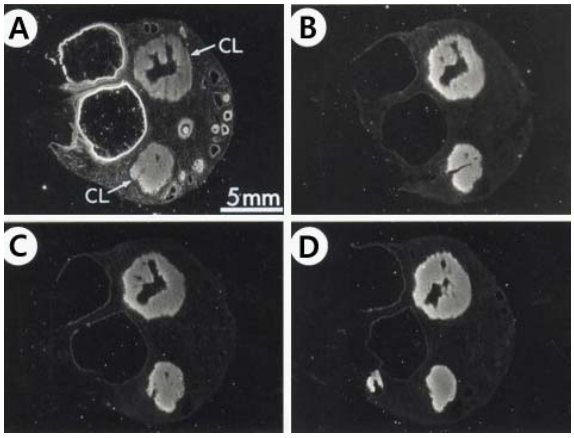

Figure 5: Dark-field photomicrograph of autoradiograms of the pig ovarian sections with corpus luteum (CL) incubated in the presence of 250 pM ^{125}I-ANP$_{(1-28)}$ (A) and its adjacent section incubated in 250 pM ^{125}I-ANP$_{(1-28)}$ plus 1 μM unlabeled ANP$_{(1-28)}$ (B), 1 μM unlabeled CNP$_{(1-22)}$ (C) or 1 μM unlabeled C-ANP (D). ^{125}I-ANP$_{(1-28)}$ binding sites appear as white silver grains

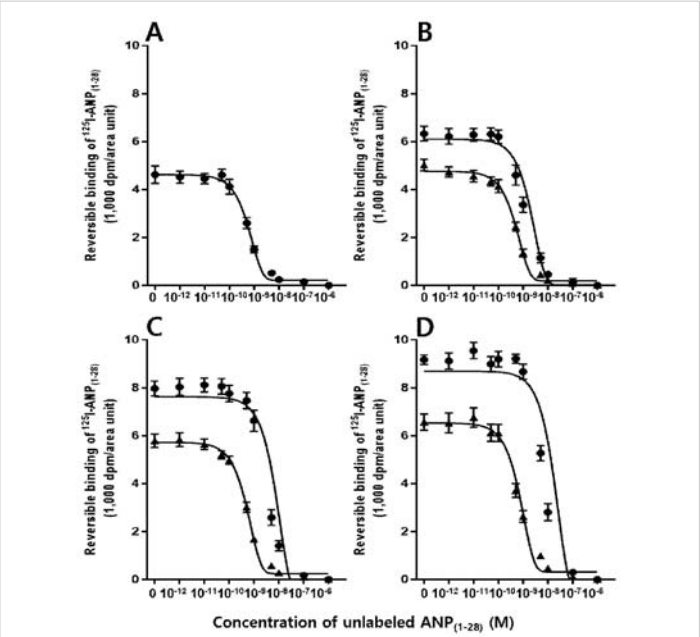

Figure 6: Competitive inhibition curves of specific ^{125}I-ANP$_{(1-28)}$ bindings to frozen sections of the pig ovary. Mean values were plotted for the competition of binding of 250 pM ^{125}I-ANP$_{(1-28)}$ to the granulosa (●) and the theca externa (▲) layers in the various sizes of follicles by increasing concentrations of unlabeled ANP$_{(1-28)}$. A, <1.0 mm; B, 1.0-1.9 mm; C, 2.0-4.0 mm; D, 4.0 mm<.

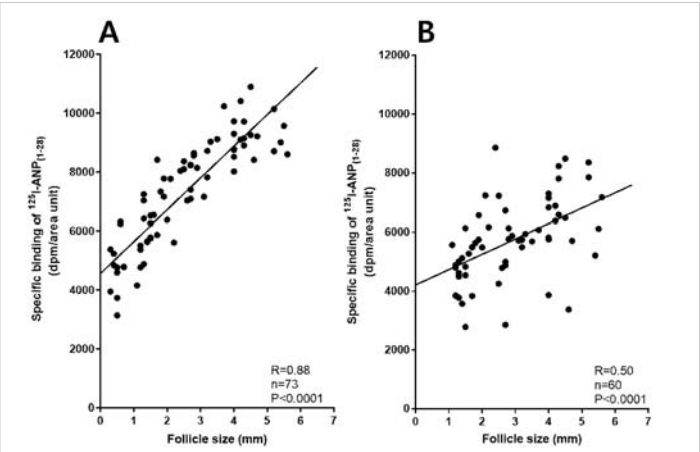

Figure 7: Correlation curve between follicle sizes and maximal specific binding densities of 250 pM ^{125}I-ANP$_{(1-28)}$ to the granulosa (A) and the theca externa (B) layers in the pig ovary.

Discussion

The present study shows the specific distribution of natriuretic peptide receptors in the ovarian follicles and their modulation in folliculogenesis.

These results clearly provide evidence for the existence of specific binding sites of ^{125}I-ANP$_{(1-28)}$ in the granulosa and theca externa layer of the antral follicles in pig ovary as well as in the granulosa layer of the primary follicles. The localization of specific ^{125}I-ANP$_{(1-28)}$ binding sites in ovarian granulosa cells was consistent with previous reports [11,12,23,24]. However, the present results demonstrate for the first time localization of specific receptors for natriuretic peptides in the theca externa layer of ovary. No specific binding sites of ^{125}I-ANP$_{(1-28)}$

Table 1: Mean values of binding constants for regionally specific reversible bindings of ^{125}I-ANP$_{(1–28)}$ in various follicles of the pig ovary.

Follicle diameter (mm)	Granulosa layer		Theca externa layer	
	K_d (nM)	B_{max} (fmol/mm^2)	K_d (nM)	B_{max} (fmol/mm^2)
< 1.0 (*n* = 13)	2.64 ± 0.75	2.32 ± 0.64	ND	ND
1.0-1.9 (*n* = 20)	2.71 ± 0.36	3.25 ± 0.38	2.61 ± 0.47	2.11 ± 0.42
2.0-4.0 (*n* = 20)	2.69 ± 0.29	5.33 ± 0.91*	1.98 ± 0.88	2.24 ± 0.36
4.0 < (*n* = 20)	2.95 ± 0.64	11.47 ± 1.27**	1.87 ± 0.93	2.31 ± 0.27

Values are means ± SE. Apparent dissociation constants (K_d) and maximum binding capacities (B_{max}) were assessed from competitive inhibition of 250 pM ^{125}I-ANP$_{(1–28)}$ binding by various concentrations of unlabeled ANP$_{(1–28)}$. ND, not detectable. *p < 0.05 and **p < 0.01 for comparison of corresponding mean values in the smallest (1.0 mm >) follicle group.

were found in the theca interna layer of any developmental stages of the follicles.

It is worthy to notice that the specific binding sites for ^{125}I-ANP$_{(1-28)}$ in the theca layer of the pig ovarian follicles were observed in the external layer but not in the internal layer. The theca of the ovarian follicle is an envelope of connective tissue surrounding the granulosa cells. It is comprised of the theca interna and theca externa. The theca interna contains theca endocrine cells; the externa is a fibrous, connective tissue layer derived from fibroblast-like cells. The theca interna/externa also contains vascular tissue, immune cells, and matrix factors. Thus, the theca layer of ovarian follicles is critical not only for maintaining the structural integrity of the follicle but also for delivering nutrients to the avascular granulosa cell layer, cumulus cells, and oocyte [25]. The gonadotropins luteinizing hormone (LH) and FSH act to stimulate theca cell and granulosa cell differentiation, respectively, in growing antral follicles. LH activates the LH receptor in theca cells, leading to increased steroidogenesis and androgen production [26]. Especially, ANP and angiotensin coexist in the ovary [27], and angiotensin II (AII) receptors also locate in the theca interna layer as well as in the granulosa cell layer of the follicles [28-30]. Therefore, the present results suggest that ANP and AII may play a possible antagonistic action for steroidogenesis and folliculogenesis within the ovarian structures.

Also, specific binding sites of ^{125}I-ANP$_{(1-28)}$ in other intra-ovarian structures including ovum, atretic follicle, corpus luteum and the other structure of the interstitium were not found in the present study using *in vitro* autoradiographic technique. Vollmar, et al. [6] have reported the presence of specific binding site for ^{125}I-ANP in the bovine corpus luteum by membrane binding assay with the crude homogenates of total corpus luteum, and also the increased production of cGMP by synthetic ANP in the corpus luteum membrane. In the present experiments, however, the specific binding site of ^{125}I-ANP$_{(1-28)}$ in the corpus luteum of pig ovary was not found. Further study remains to be confirmed whether the different properties of the binding is related to the species difference, or not.

As shown in Figures 3 and 4, the specific binding sites for ^{125}I-ANP$_{(1-28)}$ in large antral follicles are also localized in the cumulus oophorous but not in the ovum. Previous studies have reported that ANP could inhibit dose-dependently spontaneous rat oocyte maturation, and increase cGMP accumulation in oocyte-cumulus complexes without elevating cyclic adenosine monophosphate levels [31]. ANP negatively regulates FSH-activated porcine oocyte meiotic resumption, meiotic maturation and cumulus expansion. The function of ANP on porcine oocyte maturation is via the cGMP dependent protein kinase pathway [32,33]. Therefore, the present results could give good evidence for ANP functions related to the oocyte maturation in the cumulus oophorous.

In the present studies, *in vitro* autoradiography was applied in an attempt for the first time to detect the modulation of specific binding sites for ^{125}I-ANP$_{(1-28)}$ in the pig ovary with developmental stages of follicles. The specific binding sites for ^{125}I-ANP$_{(1-28)}$ in granulosa layer increased gradually in proportion to the follicular development. By analysis of the competitive inhibition by unlabeled ANP$_{(1-28)}$ of the binding of ^{125}I-ANP$_{(1-28)}$, the binding capacities of ^{125}I-ANP$_{(1-28)}$ in granulosa layer were much higher in large follicles than in small follicles. However, no significant difference of binding affinities of granulosa binding was observed in small and large follicles. A significant correlation was revealed between specific binding of ^{125}I-ANP$_{(1-28)}$ and follicle diameter in granulosa layer, however less relationship was detected in theca externa layer. These results suggest that the heterogeneity of maximal specific ^{125}I-ANP$_{(1-28)}$ binding densities in granulosa layer is related to a difference of receptor populations rather than the properties of binding affinity of the receptor molecules.

Natriuretic peptides comprise a family of 3 structurally related molecules: atrial natriuretic peptide (ANP), brain natriuretic peptide (BNP), and CNP [34]. ANP and BNP activates their cognate specific NPR-A subtype, whereas CNP stimulate NPR-B subtype. Both receptor subtypes are membrane-anchored guanylyl cyclase enzymes that signal via the production of the second messenger cGMP and undergo both homologous and heterologous desensitization, reflected by dephosphorylation of specific sites in the kinase-homology domain [35-37]. Previous studies have suggested that ovarian ANP might be involved in the regulation of follicular growth, steroidogenesis, and ovulation [7,8,31,38]. In addition to ANP, CNP has recently been found to be a follicle-stimulating factor. Zhang, et al. [13] have reported that treatment of cumulus-oocyte complexes with CNP stimulates cGMP production in cumulus cells and inhibits meiotic resumption of oocytes. Thus, CNP of granulosa and cumulus origins stimulates cGMP production by acting on its receptor in cumulus cells. Thus

these results indicate that NPR-A and NPR-B subtypes exist in granulosa and theca externa layer, although their proportional distribution of NPR subtypes in these structures are not yet defined.

In conclusion, the present study have provided autoradiographic evidence for the specific binding sites of ^{125}I-ANP in pig ovarian follicular structures; granulosa cell as well as theca externa layers. These results suggest that the intra-ovarian ANP may have physiological roles for the ovarian functions including the follicular development.

References

1. McGee EA, Hsueh AJ. Initial and Cyclic Recruitment of Ovarian Follicles. Endocr Rev. 2000; 21: 200-214. **PubMed:** https://pubmed.ncbi.nlm.nih.gov/10782364/
2. Matsuda F, Inoue N, Manabe N, Ohkura S. Follicular growth and atresia in mammalian ovaries: regulation by survival and death of granulosa cells. J Reprod Dev. 2012; 58: 44-50. **PubMed:** https://pubmed.ncbi.nlm.nih.gov/22450284/
3. Hsueh AJ, Kawamura K, Cheng Y, Fauser BC. Intraovarian control of early folliculogenesis. Endocr Rev. 2015; 36: 1-24. **PubMed:** https://pubmed.ncbi.nlm.nih.gov/25202833/
4. Potter LR, Yoder AR, Flora DR, Antos LK, Dickey DM. Natriuretic peptides: their structures, receptors, physiologic functions and therapeutic applications. Handb Exp Pharmacol. 2009; 191: 341-66. **PubMed:** https://pubmed.ncbi.nlm.nih.gov/19089336/
5. Nakagawa Y, Nishikimi T, Kuwahara K. Atrial and brain natriuretic peptides: Hormones secreted from the heart. Peptides. 2019; 111: 18-25. **PubMed:** https://pubmed.ncbi.nlm.nih.gov/29859763/
6. Vollmar AM, Mytzka C, Arendt RM, Schulz R. Atrial natriuretic peptide in bovine corpus luteum. Endocrinology. 1988; 123: 762-767.
7. Kim SH, Cho KW, Hwang YH, Oh SH, Seul KH, et al. Ovarian atrial natriuretic peptide during the rat estrous cycle. Life Sci. 1992; 51: 1291-1299. **PubMed:** https://pubmed.ncbi.nlm.nih.gov/1406049/
8. Kim SH, Cho KW, Lim SH, Hwang YH, Ryu H, et al. Presence and release of immunoreactive atrial natriuretic peptide in granulosa cells of the pig ovarian follicle. Regul Pept. 1992; 42: 153-162.
9. Ivanova MD, Gregoraszczuk EL, Augustowska K, Kolodziejczyk J, Mollova MV, et al. Localization of atrial natriuretic peptide in pig granulosa cells isolated from ovarian follicles of various size. Reprod Biol. 2003; 3: 173-181. **PubMed:** https://pubmed.ncbi.nlm.nih.gov/14666140/
10. Kim SJ, Shinjo M, Usuki S, Tada M, Miyazaki H, et al. Binding sites for atrial natriuretic peptide in high concentrations in human ovary. Biomed Res. 1987; 8: 415-420.
11. Pandey KN, Osteen KG, Inagami T. Specific receptor-mediated stimulation of progesterone secretion and cGMP accumulation by rat atrial natriuretic factor in cultured human granulosa-lutein (G-L) cells. Endocrinology. 1987; 121:1195-1197. **PubMed:** https://pubmed.ncbi.nlm.nih.gov/3040379/
12. Kim SM, Kim SH, Cho KW, Kim SY, Kim SZ. Expression of C-type natriuretic peptide and its specific guanylyl cyclase-coupled receptor in pig ovarian granulosa cells. Insights Clin Cell Immunol. 2018; 2: 14-25. **PubMed:** https://www.heighpubs.org/hcci/icci-aid1004.php
13. Zhang M, Su YQ, Sugiura K, Xia G, Eppig JJ. Granulosa cell ligand NPPC and its receptor NPR2 maintain meiotic arrest in mouse oocytes. Science. 2010; 330: 366-369. **PubMed:** https://pubmed.ncbi.nlm.nih.gov/20947764/
14. Zhang M, Su YQ, Sugiura K, Wigglesworth K, Xia G, et al. Estradiol promotes and maintains cumulus cell expression of natriuretic peptide receptor 2 (NPR2) and meiotic arrest in mouse oocytes in vitro. Endocrinology. 2011; 152: 4377-4385. **PubMed:** https://pubmed.ncbi.nlm.nih.gov/21914782/
15. Liu L, Kong N, Xia G, Zhang M. Molecular control of oocyte meiotic arrest and resumption. Reprod Fertil Dev. 2013; 25: 463-471. **PubMed:** https://pubmed.ncbi.nlm.nih.gov/23217677/
16. Brown J, Chen Q. Regional expression of natriuretic peptide receptors during the formation of arterial neointima in the rabbit. Circ Res. 1995; 77: 906-918. **PubMed:** https://pubmed.ncbi.nlm.nih.gov/7554144/
17. Cho KW, Kim SH, Kim CH, Koh GY. Mechanical basis of ANP secretion in beating atria: atrial stroke volume and ECF translocation. Am J Physiol. 1995; 268: R1129-R1136. **PubMed:** https://pubmed.ncbi.nlm.nih.gov/7771572/
18. Joseph LJ, Desai KB, Mehta MN, Mathiyarasu R. Measurement of specific activity of radiolabelled antigens by a simple radioimmunoassay technique. Nucl Med Biol. 1988; 15: 589-590. **PubMed:** https://pubmed.ncbi.nlm.nih.gov/3254882/
19. Brown J, Zuo Z. Natriuretic peptide receptors in the fetal rat. Am J Physiol. 1995; 269: E261-273. **PubMed:** https://pubmed.ncbi.nlm.nih.gov/7653646/
20. Kim SZ, Kim SH, Cho KW. Overlapping distribution of receptors for atrial natriuretic peptide and angiotensin II in the kidney and the adrenal gland of the freshwater turtle, Amyda japonica. Gen Comp Endocrinol. 1997; 108: 119-131. **PubMed:** https://pubmed.ncbi.nlm.nih.gov/9378266/
21. Benfenati F, Cimino M, Agnati LF, Fuxe K. Quantitative autoradiography of central neurotransmitter receptors: methodological and statistical aspects with special reference to computer-assisted image analysis. Acta Physiol Scand. 1986; 128: 129-146. **PubMed:** https://pubmed.ncbi.nlm.nih.gov/3022554/
22. Munson PJ, Rodbard D. Ligand: a versatile computerized approach for characterization of ligand-binding systems. Anal Biochem. 1980; 107: 220-239. **PubMed:** https://pubmed.ncbi.nlm.nih.gov/6254391/
23. Zhang W, Yang Y, Liu W, Chen Q, Wang H, et al. Brain natriuretic peptide and C-type natriuretic peptide maintain porcine oocyte meiotic arrest. J Cell Physiol. 2015; 230: 71-81. **PubMed:** https://pubmed.ncbi.nlm.nih.gov/24912131/
24. Noubani A, Farookhi R, Gutkowska J. B-type natriuretic peptide receptor expression and activity are hormonally regulated in rat ovarian cells. Endocrinology. 2000; 141: 551-559. **PubMed:** https://pubmed.ncbi.nlm.nih.gov/10650935/
25. Young JM, McNeilly AS. Theca: the forgotten cell of the ovarian follicle. Reproduction. 2010; 140: 489–504. **PubMed:** https://pubmed.ncbi.nlm.nih.gov/20628033/
26. Richards JS, Ren YA, Candelaria N, Adams JE, Rajkovic A. Ovarian Follicular Theca Cell Recruitment, Differentiation, and Impact on Fertility: 2017 Update. Endocr Rev. 2018; 39: 1-20. **PubMed:** https://pubmed.ncbi.nlm.nih.gov/29028960/
27. Usuki S, Saitoh T, Saitoh M, Tanaka J, Kawakura Y, et al. Endothelin-renin-angiotensin-atrial natriuretic peptide system in ovaries: an intraovarian ERAANP system. J Cardiovasc Pharmacol. 1993; 22 Suppl 8: S207-210. **PubMed:** https://pubmed.ncbi.nlm.nih.gov/7509946/
28. Husain A, Bumpus FM, De Silva P, Speth RC. Localization of angiotensin II receptors in ovarian follicles and the identification of angiotensin II in rat ovaries. Proc Natl Acad Sci U S A. 1987; 84: 2489-2493. **PubMed:** https://pubmed.ncbi.nlm.nih.gov/3470807/
29. Speth RC, Bumpus FM, Husain A. Identification of angiotensin II receptors in the rat ovary. Eur J Pharmacol. 1986; 130: 351-352. **PubMed:** https://pubmed.ncbi.nlm.nih.gov/3792456/

30. Gonçalves PB, Ferreira R, Gasperin B, Oliveira JF. Role of angiotensin in ovarian follicular development and ovulation in mammals: a review of recent advances. Reproduction. 2012; 143: 11-20.
PubMed: https://pubmed.ncbi.nlm.nih.gov/22046052/

31. Tornell J, Carlsson B, Billig H. Atrial natriuretic peptide inhibits spontaneous rat oocyte maturation. Endocrinology. 1990; 126: 1504-1508.
PubMed: https://pubmed.ncbi.nlm.nih.gov/2155102/

32. Zhang M, Tao Y, Xia G, Xie H, Hong H, et al. Atrial natriuretic peptide negatively regulates follicle-stimulating hormone-induced porcine oocyte maturation and cumulus expansion via cGMP-dependent protein kinase pathway. Theriogenology. 2005; 64: 902-916.
PubMed: https://pubmed.ncbi.nlm.nih.gov/16054495/

33. Zhang M, Tao Y, Zhou B, Xie H, Wang F, et al. Atrial natriuretic peptide inhibits the actions of FSH and forskolin in meiotic maturation of pig oocytes via different signalling pathways. J Mol Endocrinol. 2005; 34: 459-472.
PubMed: https://pubmed.ncbi.nlm.nih.gov/15821110/

34. Brenner BM, Ballermann BJ, Gunning ME, Zeidel ML. Diverse biological actions of atrial natriuretic peptide. Physiol Rev. 1990; 70: 665-699.
PubMed: https://pubmed.ncbi.nlm.nih.gov/2141944/

35. Koller KJ, Lowe DG, Bennett GL, et al. Selective activation of the B natriuretic peptide receptor by C-type natriuretic peptide (CNP). Science. 1991; 252: 120-123.
PubMed: https://pubmed.ncbi.nlm.nih.gov/1672777/

36. Tremblay J, Desjardins R, Hum D, Gutkowska J, Hamet P. Biochemistry and physiology of the natriuretic peptide receptor guanylyl cyclases. Mol Cell Biochem. 2002; 230: 31-47.
PubMed: https://pubmed.ncbi.nlm.nih.gov/11952095/

37. Schulz S. C-type natriuretic peptide and guanylyl cyclase B receptor. Peptides. 2005; 26: 1024-1034.
PubMed: https://pubmed.ncbi.nlm.nih.gov/15911070/

38. Steegers EA, Hollanders JM, Jongsma HW, Hein PR. Atrial natriuretic peptide and progesterone in ovarian follicular fluid. Gynecol Obstet Invest. 1990; 29: 185-187.
PubMed: https://pubmed.ncbi.nlm.nih.gov/2141584/